Cell

The Ribosome as an Optimal Decoder: A Lesson in Molecular Recognition

Yonatan Savir[1] and Tsvi Tlusty[2,*]
[1]Department of Systems Biology, Harvard Medical School, Boston, MA 02115, USA
[2]The Simons Center for Systems Biology, Institute for Advanced Study, Princeton, NJ 08540, USA
*Correspondence: tlusty@ias.edu
http://dx.doi.org/10.1016/j.cell.2013.03.032

SUMMARY

The ribosome is a complex molecular machine that, in order to synthesize proteins, has to decode mRNAs by pairing their codons with matching tRNAs. Decoding is a major determinant of fitness and requires accurate and fast selection of correct tRNAs among many similar competitors. However, it is unclear whether the modern ribosome, and in particular its large conformational changes during decoding, are the outcome of adaptation to its task as a decoder or the result of other constraints. Here, we derive the energy landscape that provides optimal discrimination between competing substrates and thereby optimal tRNA decoding. We show that the measured landscape of the prokaryotic ribosome is sculpted in this way. This model suggests that conformational changes of the ribosome and tRNA during decoding are means to obtain an optimal decoder. Our analysis puts forward a generic mechanism that may be utilized broadly by molecular recognition systems.

INTRODUCTION

Proteins are synthesized by the ribosome, an intricate molecular machine that decodes the genetic blueprint of the messenger RNA (mRNA) and polymerizes the corresponding amino acids carried by transfer RNAs (tRNAs) into a protein (Bashan and Yonath, 2008). Protein biosynthesis relies on the quality and efficiency of mRNA decoding, that is on the ability of the ribosome to select the correct (cognate) aminoacyl-tRNAs and reject the wrong (noncognate) ones. In its function as a molecular decoder, the ribosome utilizes the differences in specific binding energy between the cognate and noncognate tRNAs. The free energy differences due to base pair mismatches between the mRNA codon and the tRNA anticodon are too small to provide the observed high accuracy of tRNA selection (Ogle and Ramakrishnan, 2005; Xia et al., 1998), even if kinetic proofreading (Hopfield, 1974; Ninio, 1975) is taken into account. Additional specific binding energy is gained from the interaction between the minor groove of the codon-anticodon helix and the ribosome decoding center (Ogle et al., 2001). Several studies found evidence for significant conformational changes during decoding (Pape et al., 1999), including a domain closure in the 30S subunit (Demeshkina et al., 2012; Ogle et al., 2002) and distortion of the tRNA (Demeshkina et al., 2012; Schmeing et al., 2009; Schuette et al., 2009; Villa et al., 2009).

The decoding pathways of cognate and near-cognate tRNAs are multistep processes (Figure 1A) whose rates have been measured by pre-steady-state kinetics and single-molecule fluorescence resonance energy transfer (FRET) experiments (Blanchard et al., 2004; Gromadski et al., 2006; Gromadski and Rodnina, 2004a; Lee et al., 2007; Marshall et al., 2008; Rodnina and Wintermeyer, 2001; Zaher and Green, 2010). Structural and kinetic data, combined with energy landscape calculations (Ferreiro et al., 2011; Schug and Onuchic, 2010), suggest that the translation process involves an intricate energy landscape with multiple metastable states (Munro et al., 2009; Whitford et al., 2010a, 2010b, 2011a, 2011b). The structural and energetic parameters (Figure 1B) that characterize each step in the measured landscape may be coupled, thus leading to possible tradeoffs, for example between the speed and accuracy of decoding (Johansson et al., 2008; Ninio, 2006). This raises the question as to whether the observed ribosome parameters have evolved to provide effective decoding, or perhaps they are biochemically constrained (Johansson et al., 2008, 2011).

These questions regarding adaptation versus constraints and regarding possible tradeoffs are general ones and are relevant in many other molecular recognition systems. Examples include antibodies targeting antigens, regulatory proteins binding to DNA, and enzymes catalyzing their substrate, which all require recognition of specific targets within a noisy background of similar competing molecules. We therefore put our examination of tRNA decoding by the ribosome into the context of the general recognition problem, which we discuss below in terms of standard enzymatic kinetics (Michaelis-Menten). We show that the conclusions from the analysis of the ribosome can be directly applied to the generic molecular recognition system.

Previous studies of protein recognition (Fersht, 1998; Herschlag, 1988; Post and Ray, 1995; Savir and Tlusty, 2007) and of tRNA recognition by the ribosome (Johansson et al., 2008, 2011, 2012; Ninio, 2006) focused mainly on the ratio between the rates of the competing reactions, commonly termed *specificity* or *accuracy*, as a measure for recognition quality. In the case of the ribosome, as well as many other recognition schemas, rate and specificity are negatively correlated. Several studies gave insight on how the effective kinetic parameters

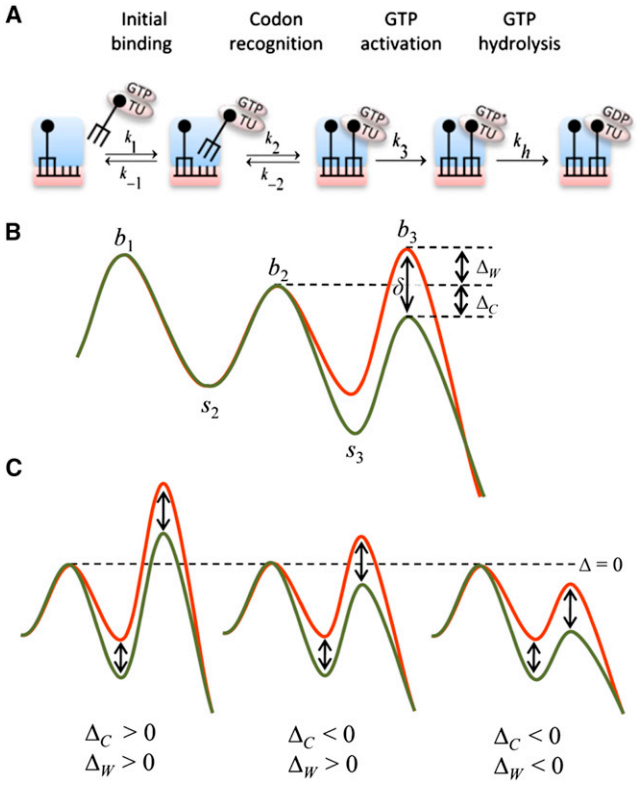

Figure 1. The Multistage Kinetics of Decoding by the Ribosome

(A) The decoding reaction, which is followed by kinetic proofreading, contains several basic stages: initial binding, codon recognition, GTP activation, and GTP hydrolysis. Initial binding and codon recognition—a complex of elongation factor (EF-Tu), GTP, and aminoacyl-tRNA binds to the ribosome. Codon is recognized by pairing with the anticodon and by additional interaction of the decoding center with the codon-anticodon minor groove in a manner that is sensitive to Watson-Crick geometry, but not to base sequence. As a result, cognate tRNAs are more stable than noncognate ones. GTP activation and hydrolysis—codon recognition leads to global conformational changes of the ribosome and tRNA, which are different for cognate or noncognate tRNAs and play a role in GTP activation and hydrolysis by EF-Tu.

(B) The free energy landscape of codon recognition as suggested by experiments. In the stages that are sensitive to codon identity, the correct (green) and wrong (red) pathways split (s_3 and b_3). The tRNA specific parameters are the dissociation rate of the codon-anticodon complex (k_{-2}) and the forward rate of GTP activation (k_3).

(C) The three possible regimes of the decoding energy landscape correspond to three regimes of the barrier differences, Δ_C and Δ_W, where *C* and *W* denote correct and wrong, respectively (for given specific differences, arrows).

affect the rate and specificity. For example, reaction rate can be maximized via strong binding of the enzyme to the transition state of the substrate rather than to the initial state (Fersht, 1998; Herschlag, 1988), whereas specificity can be optimized by tuning system parameters, such as the energy barriers of conformational changes (Post and Ray, 1995; Savir and Tlusty, 2007, 2008, 2009, 2010). Yet, a coherent understanding of what should be the *resolution* of the rate-specificity tradeoff is still missing, and it is not clear whether such an optimal design can withstand varying conditions. In this work, we present a general solution to the problem of balancing the tradeoff between correct and incorrect rates of competing reactions. To this end, we take into account the effect of all kinetic parameters, not only effective ones, and analyze a general measure (or "fitness" function). The only constraint on the fitness is that it increases with the correct rate and decreases with the incorrect one.

By analyzing the performance of the ribosome as a decoder, we derive the rate constants and the corresponding energy landscape that provide optimal balance between the decoding rate and the ability to discriminate between two competing substrates. We find that the measured energy landscape of the ribosome is nearly optimal for decoding, suggesting that the reaction energetics and conformational changes have coevolved to ensure optimal decoding. Although we previously examined the specific case of competitive binding (Savir and Tlusty, 2010), here we treat the general recognition problem, taking into account the entire energy landscape of the reaction pathways and a general fitness function. Our treatment thus shows that the utilization of conformational changes to enhance recognition is a general mechanism that does not depend on the specific form of the fitness function. Because the kinetic scheme of the ribosome is equivalent to the generic enzyme kinetics, this mechanism has the potential of being widely utilized by almost any molecular recognition system that has to efficiently discern between competing ligands.

RESULTS

The tRNA Decoding Pathway

Figure 1A depicts a three-step scheme as deduced from kinetic studies (Johansson et al., 2008)—initial binding, which is insensitive to the identity of the incoming codon, followed by codon-specific binding and guanosine triphosphate (GTP) activation. This kinetics can be described in terms of a free energy landscape, which is shaped by varying five parameters (Figure 1B): the two stable intermediate states s_2 and s_3 and the three barriers b_1, b_2, and b_3 (in units of k_BT, the initial state is at zero level). The rate of decoding correct tRNAs at steady state, R_C (per ribosome per tRNA), depends solely on the three barriers and is inversely proportional to the sum of their exponents (Experimental Procedures),

$$R_C \propto \frac{1}{e^{b_1}+e^{b_2}+e^{b_3}} = \frac{1}{e^{B}+e^{b_3}}, \qquad \text{(Equation 1)}$$

where B is defined by $e^B \equiv e^{b_1}+e^{b_2}$. The dependence of the rates on the stable states cancels off because shifting these states merely varies the backward and forward rates by the same factor. The difference between correct (cognate) and wrong (noncognate) codons is in the dissociation rate of the codon-anticodon complex (k_{-2}) and in the forward rate of GTP activation (k_3). The resulting rate of decoding wrong tRNAs, R_W, is

$$R_W \propto \frac{1}{e^{b_1}+e^{b_2}+e^{b_3+\delta}} = \frac{1}{e^{B}+e^{b_3+\delta}}, \qquad \text{(Equation 2)}$$

where δ is the difference between the GTP activation barriers of the correct and wrong reactions (Figure 1B). Hereafter, the subscripts *C* and *W* denote correct and wrong, respectively.

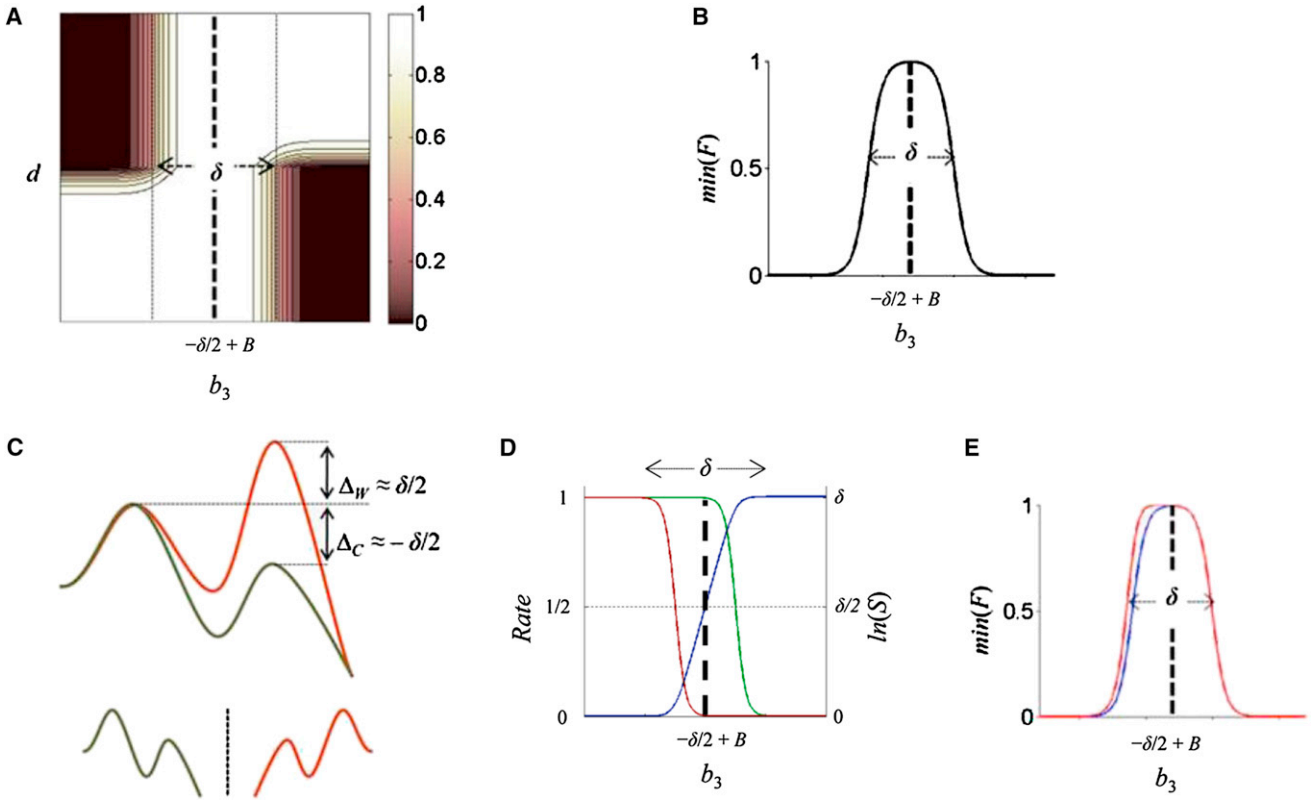

Figure 2. The Optimal Landscape

(A) The fitness $F \propto R_C - d \cdot R_W$ (normalized by its maximum for every given value of sensitivity d, color bar) as a function of the barrier b_3 and d. When d is large, the wrong decoding rate is dominant, and thus the optimal b_3 is high. At the other extreme, when d is small, the optimal b_3 is low.

(B) The minimal value of F for a given b_3 ("worst-case scenario"). The optimal barrier, the "max-min strategy," $b_3 = -\delta/2 + B$, provides more than 95% of the maximal possible fitness for any d. A "band" of beneficial values of width $\sim \delta$ is centered around this optimal barrier.

(C) Top: optimal landscape in terms of the barrier differences Δ. For $|\ln(\rho)| \ll \delta$, which is the case for the ribosome, the optimal design (Equation 3) is symmetric; i.e., $\Delta_C^* = -\Delta_W^* \approx -\delta/2$. Bottom: the symmetric optimum implies that the ratio of forward and backward rates is inverted between the correct and wrong energy landscapes, $(k_3/k_{-2})_C = (k_{-2}/k_3)_W$.

(D) The correct decoding rate, R_C (green), wrong decoding rate, R_W (red), and the logarithm of the specificity, $S = R_C/R_W$, as function of b_3. In the region of the max-min solution, the correct rate is near its maximal value, whereas the wrong rate is almost zero. The optimal specificity S^* is roughly the square root of the maximal possible value, $S^* = S_{\max}^{1/2}$.

(E) This solution is also the min-max strategy for various fitness functions, such as $F \propto R_C - d \cdot (R_W/R_C)$ (blue) and $F \propto R_C - d \cdot R_W^2$ (red).

Rate-Specificity Tradeoff in Enzymes

The Michaelis-Menten (MM) scheme is a generic enzymatic scheme describing a variety of biological processes (Fersht, 1985) and is sometimes used to model tRNA decoding (Johansson et al., 2008; Ninio, 2006). The MM scheme consists of two basic steps: a reversible binding-unbinding step with rates k_{on} and k_{off}, respectively, followed by an irreversible "catalysis" step with a rate k_{cat}. The rate of the overall reaction, per substrate per enzyme, is $R = k_{cat}k_{on}/(k_{cat} + k_{off}) = k_{cat}/K_M$, where $K_M = (k_{cat} + k_{off})/k_{on}$ is the MM constant. The tRNA decoding rates (Equations 1 and 2) may also describe the MM kinetics when the barriers b_1 and b_2 are merged (Figure 1B), and the height of the combined barrier is set to B (Extended Experimental Procedures). Hence, all our following results that are demonstrated and tested for ribosomes can be applied to any recognition system described by MM kinetics. For simplicity and, because this is the case for the ribosome, we assume competing reactions with the same association rate k_{on}. Some aspects of the general case are discussed in the Extended Experimental Procedures.

A traditional measure of accuracy is the specificity $S = R_C/R_W = (k_{cat}/K_M)_C/(k_{cat}/K_M)_W$ (Fersht, 1998). From Equations 1 and 2, it follows that S and the correct decoding rate R_C are negatively correlated (Johansson et al., 2008): $R_C \propto (e^{\delta} - S)/(e^{\delta} - 1)$. It is evident that specificity approaches its maximal value $S_{\max} = e^{\delta}$ when the rate vanishes $R_C = 0$, whereas the rate is maximal when the specificity is minimal $S_{\min} = 1$ (Figure 2D). This relation merely expresses a constraint that follows directly from the definition of the MM or ribosome decoding schemes. However, it cannot predict where the optimal recognition or decoding regime resides along the curve. This is exactly the question that we address in this work: how to tune the kinetic parameters in order to achieve a fast correct reaction (high R_C) while retaining high specificity (high

$S = R_C/R_W$). Or, in terms of the equivalent energy landscape, what are the energy barriers that lead to optimal molecular recognition?

General Properties of the Fitness Function

The ribosome is an important example for a molecular recognition system that needs to balance between the costs and benefits of correct and incorrect recognition. This interplay may be quantitatively described as optimizing a performance measure ("fitness"), which is a function of the correct and wrong decoding rates, $F(R_C,R_W)$. For a general molecular recognition system, the exact form of F is unknown or depends on the biological context and environmental conditions. Because the decoding rates (Equations 1 and 2) describe a general recognition system, we discuss first the generic properties of the fitness function $F(R_C, R_W)$ and then investigate the performance of the ribosome. F is not limited to any specific form, and the only requirement is that it makes sense as a fitness function ("biologically reasonable")—namely, increasing the correct rate increases F, $\partial F/\partial R_C>0$, while increasing the incorrect rate decreases F, $\partial F/\partial R_W<0$.

We show that, for any such fitness function F, increasing the specific discrimination energy δ always increases F (Experimental Procedures). Thus, F obtains its maximal value at the upper limit of δ. Moreover, there are two possibilities for an extremum in F: either an extremum as a function of b_3, which is reached at the lower limit of B, or an extremum as a function of B, which is reached at the upper limit of b_3. Hence, optimizing the fitness becomes a one-dimensional problem because only one parameter, b_3 or B, has an "optimal" value, whereas the other parameter is expected to approach its biophysical limit.

The Decoding Fitness Function

A standard example for a fitness function is the performance measure of manmade decoders (Helstrom, 1995) which is the weighted difference between the rates of correct and wrong decisions, $F \propto [t_C]R_C - r\cdot[t_W]R_W$, where $[t_C]$ and $[t_W]$ are the concentrations of the correct and incorrect tRNA, respectively. The weight r accounts for the relative impact of correct or wrong transmission on the system. The aim of an engineer is to maximize this merit function (or "decoding fitness"). In terms of the ribosome energy barriers, the decoding fitness function F takes the form $F \propto 1/(e^B + e^{b_3}) - d/(e^B + e^{b_3+\delta})$, where $d = r\cdot[t_W]/[t_C]$ is the sensitivity of the decoding system to errors, taking into account the abundance of cognate and noncognate tRNAs.

In the case of decoding fitness, the extremum point in the B direction is always a minimum, and the fitness obtains its maximal value at the point where the first derivate of b_3 vanishes, δ reaches its upper boundary, and B reaches its lower boundary (Experimental Procedures). In other words, both B and δ are expected to reach their biophysical limits, and the one parameter that is left to optimize is b_3. Figure 1C depicts possible designs of the decoding energy landscape that correspond to different values of b_3. It is convenient to graph the landscape also in terms of the barrier difference $\Delta = b_3 - b_2$ (Figures 1B and 1C). This experimentally accessible quantity is the logarithm of the ratio between the backward rate from the codon recognition stage (k_{-2}) and the forward GTP activation rate (k_3). Thus, the three possible design regimes (Figure 1C) are characterized by different "forward" to "backward" ratios.

We can now rephrase the main question of this study in terms of the energy landscape: (1) what is the optimal barrier b_3 (or Δ)? (2) Does the ribosome exhibit such optimality? (3) What is then the role of conformational changes?

Symmetric Energy Landscape Provides Optimal Decoding

To address this question, we first maximized the decoding fitness F with respect to b_3, for given values of B and δ (Experimental Procedures). We showed that, for a very wide range of d, the sensitivity of the decoding system to errors, there exists an optimal barrier b_3 that maximizes F. This result can be generalized to any biologically reasonable fitness function—an optimal barrier exists as long as both R_C and R_W are relevant to the fitness F, i.e., $\partial F/\partial R_C$ and $\partial F/\partial R_W$ are not different by too many orders of magnitude. Moreover, this optimal value of the barrier is always in the region in between the steepest points of R_C and R_W (Figure 2).

The barrier that maximizes decoding depends on the value of the sensitivity d (Experimental Procedures). However, the actual, biologically relevant values of d are unknown and can only be roughly estimated. Moreover, d is expected to vary because tRNA concentrations and the relative significance of correct and wrong decoding depend on environmental and physiological conditions. We therefore examine optimality as d is varied (Figure 2A). We find the solution that ensures that the minimal fitness for all values of d (the "worst-case scenario") is the maximal possible one (a "max-min strategy"). The optimal barriers for correct and wrong tRNAs are $b^*_{3C} = -\delta/2 + B$ and $b^*_{3W} = +\delta/2 + B$, respectively (Experimental Procedures and Extended Experimental Procedures). For any value of d, this solution provides more than 95% of the maximal possible fitness (Figures 2A and 2B).

To compare this prediction with measurements, it is convenient to present the fitness and rates as a function of $\Delta = b_3 - b_2$ (Figure 1C). The optimal correct and wrong barrier differences of the max-min solution are (Experimental Procedures)

$$\Delta^*_C = -\frac{1}{2}\delta - \ln p,$$
$$\Delta^*_W = +\frac{1}{2}\delta - \ln p. \qquad \text{(Equation 3)}$$

where $p = k_{-1}/(k_{-1}+k_2)$ is the probability of a tRNA to be rejected from the state of initial binding. For $|\ln(p)| \ll \delta$, which is the case for the ribosome, the model predicts that the optimal design is symmetric (Figure 2C), i.e., $\Delta^*_C = -\Delta^*_W \approx -\delta/2$. The symmetric optimum implies that the ratio of forward and backward rates is inverted between the correct and wrong energy landscapes, $(k_3/k_{-2})_C = (k_{-2}/k_3)_W$.

The Specificity in the Optimal Regime Is Smaller Than the Maximal One

In the region of the max-min solution, the optimal specificity S^* is roughly the square root of the maximal possible value,

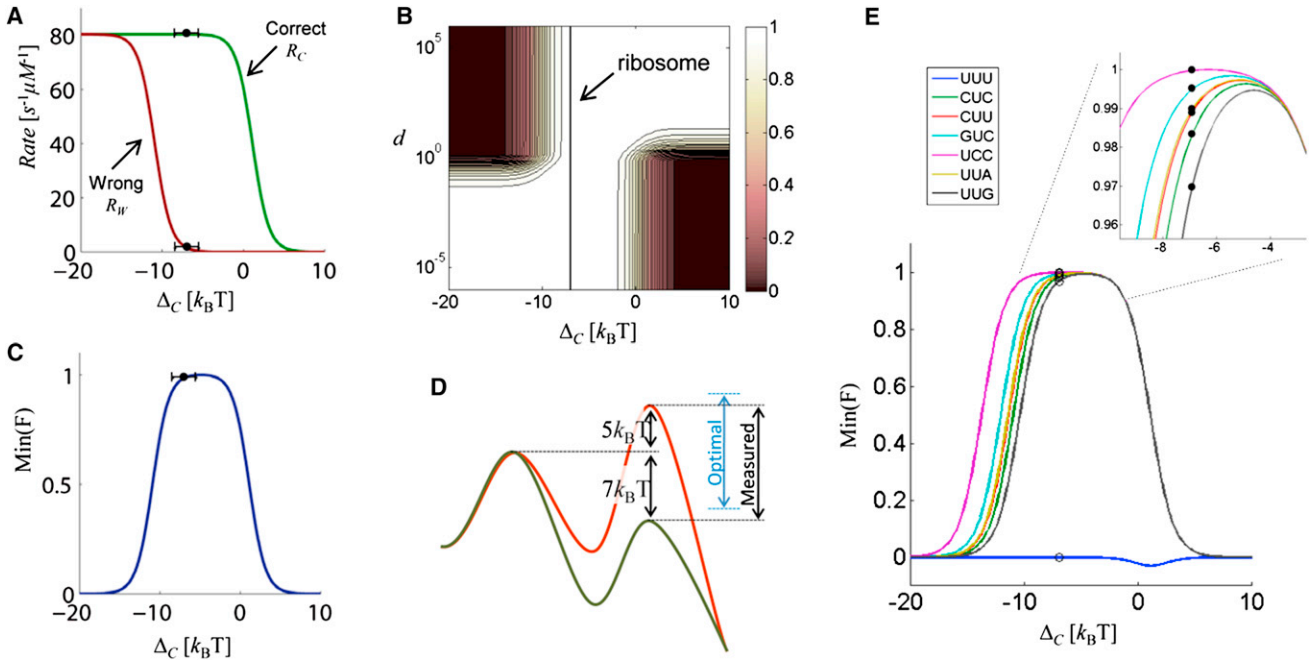

Figure 3. The Measured Prokaryotic Ribosome Is a Nearly Optimal Decoder

(A) The decoding rates, per ribosome and per tRNA, for correct (UUC) and wrong (CUC) codons are sigmoidal functions of the barrier difference Δ_C, plotted for measured values $p = 0.3 \pm 0.04$ and $\delta = 12 \pm 2.0 k_B T$ (Gromadski et al., 2006; Gromadski and Rodnina, 2004a) (Supplemental Information, Table S1). The black dot is the measured correct barrier difference, $\Delta_C = -7 \pm 1.4 k_B T$. The uncertainty is derived using the SD in measurement of the rate constants (Supplemental Information, Table S1).

(B) The decoding fitness (normalized by its maximum for every given value of sensitivity d, color bar) as a function of the correct barrier difference Δ_C and d. The black line is the measured Δ_C.

(C) The minimal value of F for a given Δ_C. The measured value of Δ_C (black dot) puts the ribosome within the optimal regime.

(D) The actual measured landscape for the ribosome is similar to the optimal design.

(E) Results for six non-cognate codons for the cognate codon UUC (Gromadski et al., 2006; Gromadski and Rodnina, 2004a). The decoding is optimal for all codons, except for UUU which carries the same amino-acid as UUC. *Inset*: a zoom at the optimal region.

$S^* = R_C/R_W = e^{\delta/2} = S_{\max}^{1/2}$ (Figure 2D). The value of S^* is the outcome compromising the conflicting needs for maximal rate and maximal specificity. It may seem somewhat counterintuitive that molecular recognition compromises specificity exactly in the presence of a competing reaction. The reason is the need to retain high enough rate of correct reaction, which is critical for the ribosome. Indeed, around the max-min solution, the correct rate is close to its maximal value $R_C^* \propto 1/(1+e^{-\delta/2})$. This suggests that, in some cases, the need for amplification of the specificity via kinetic proofreading stems from a relatively low nominal specificity. An additional kinetic proofreading step approximately squares the specificity (Hopfield, 1974; Ninio, 1975) and thus can recover the maximal specificity $(S^*)^2 = S_{\max}$. This result implies that enzymes with competing substrates, which have roughly the same association constant, do not operate at the regime of maximal specificity but at approximately a square root of this value.

Optimality Holds for a Wide Range of Fitness Functions

The optimal design (Equation 3) holds also for other forms of fitness. A plausible requirement from an optimal decoder examined above is minimizing the incorrect rate R_w. However, it is also possible that the relevant quantity to be minimized is the error rate R_w/R_c, with a fitness function $F = R_C - d \cdot R_W/R_C$. The optimal solution above holds also for this form of F, as well as to other forms, such as $F = R_C - d \cdot R_W^2$ (Figure 2E). In fact, we show that an optimal solution exists for any biologically reasonable fitness $F(R_C, R_W)$, as long as both R_w and R_c are relevant variables (i.e., the derivatives $\partial F/\partial R_C$ and $\partial F/\partial R_W$ are not different by many orders of magnitude [Experimental Procedures]). Furthermore, our conclusion remains valid, even with additional reversible stages (Lee et al., 2007) (because these do not affect the steady-state fluxes), or if the first two stages (initial binding and codon recognition) are combined (Johansson et al., 2008; Ninio, 2006).

The Experimentally Measured Landscapes Are Nearly Symmetric

In experiments in which the cognate codon was UUC and the near-cognate codon was CUC, the measured parameters were $p \approx 0.3$ and $\delta \approx 12\, k_B T$, whereas the measured correct and wrong barrier differences are $\Delta_C^* \approx -7\, k_B T$ and $\Delta_W^* \approx 5\, k_B T$ (Gromadski et al., 2006; Gromadski and Rodnina, 2004a) (Supplemental Information; Table S1). The measured values place the ribosome well within the symmetric, optimal regime predicted by theory (Figures 3A–3D). We further examined the optimality prediction in measurements of the discrimination between UUC and six additional noncognate codons (Gromadski et al.,

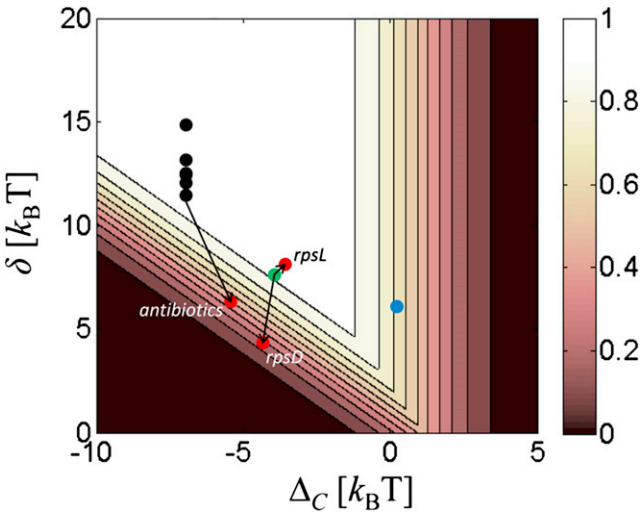

Figure 4. Optimality in the Space of Energy Landscapes

The normalized fitness of the max-min solution (Figure 3C; Equation 11) as a function of the specific difference between the cognate and noncognate codons, δ, and the cognate energy barrier difference, Δ_C. The fitness increases monotonically with δ. Per a given value of the specific difference δ, there is an optimal value for the energy barrier difference Δ_C around –δ/2 (in a band $-\delta \le \Delta_C \le 0$). The results of pre-steady-state kinetics (black circles [Gromadski et al., 2006; Gromadski and Rodnina, 2004a], green circle [Zaher and Green, 2010]) and FRET experiment (blue circle [Lee et al., 2007]) (Supplemental Information; Tables S1, S2, S3, and S4) indicate that the *E. coli* ribosome is in this optimal region. Arrows indicate a measurement of mutated ribosomes (*rpsL* and *rpsD* [Zaher and Green, 2010]) or the effect of antibiotics (streptomycin [Gromadski and Rodnina, 2004b]; see also Supplemental Information, Table S2, and Figure S1). Theory predicts that ribosomes of other organisms will also reside in this optimal regime.

2006) (Figure 3E). We find that the cognate/noncognate decoding is nearly optimal for all of these codons. One exception is UUU, which is the only codon besides UUC that encodes the amino acid phenylalanine. In this case, the discrimination is poor ($F \approx 0$) because the ribosome should not reject UUU, which carries the correct amino acid.

DISCUSSION

Deformation Enhances the Decoding by the Ribosome

It has been suggested that the conformational changes of the ribosome and the tRNA play a crucial role in determining decoding accuracy (Demeshkina et al., 2012; Frank et al., 2005; Ogle et al., 2002; Ogle and Ramakrishnan, 2005; Pape et al., 1999; Schmeing and Ramakrishnan, 2009; Schmeing et al., 2009; Schuette et al., 2009; Villa et al., 2009; Yarus et al., 2003). To quantitatively examine the role of conformational changes, we derive a criterion that indicates when deformation becomes beneficial. We divide the barrier Δ_C into free energy gained from binding, ΔG_B, (e.g., Watson-Crick pairing and minor groove interaction) and free energy invested in deformation, ΔG_D, $\Delta_C = \Delta G_D - \Delta G_B$. In the optimal regime (Equation 3),

$$\Delta G_D = \Delta G_B - \frac{1}{2}\delta - \ln p. \qquad \text{(Equation 4)}$$

This implies that, as long as the binding energy is larger than a rather moderate value, $\Delta G_B \ge \delta/2 + \ln p \approx 5 k_B T$, optimal decoding requires positive deformation energy; i.e., deformations during decoding are beneficial. We therefore suggest that optimality is obtained by tuning, via coevolution, the binding and deformation energies within the physical regime dictated by the constraints on the ribosome and the tRNA.

Investing deformation energy to enhance discrimination appears as a general strategy of molecular recognition systems. This strategy, termed conformational proofreading (Savir and Tlusty, 2007, 2008, 2009, 2010), provides a concrete underlying mechanism, which explains how these deformations are utilized to achieve optimal decoding landscape. Conformational proofreading was demonstrated in the specific case of homologous search (Savir and Tlusty, 2010; De Vlaminck et al., 2012) for a specific linear form of fitness function (weighted difference). Here, we proved the existence of an optimal energy landscape for any biologically reasonable fitness, one that increases with R_C and decreases with R_W. We showed that this general conclusion applies to the ribosome, as well as to the generic MM kinetics in the presence of competition.

Theory Predicts Optimal Regime of Ribosomes in Other Organisms

During protein synthesis, incorrect amino acids might be incorporated due to errors in tRNA aminoacylation or tRNA selection by the ribosome. The in vivo misincorporation rate has been estimated to be in the range of 6×10^{-4}–5×10^{-3} errors per amino acid (Bouadloun et al., 1983). The observation that incorrect aminoacylation occurs at a rate of 10^{-4}–10^{-5} suggests that protein integrity largely depends on the ribosome decoding performance (Zaher and Green, 2009). Protein sequence is crucial for their fold and function, and translation errors might therefore be deleterious to the cell. For example, mutating the elongation factor TU (EF-TU) in bacteria doubled the error rate and slowed down growth by 10%, whereas a fourfold increase in error rate led to growth that was slower by 30% (Ehrenberg and Kurland, 1984; Kurland, 1992). Another example is ribosomal ambiguity mutants (ram) with altered ribosomal proteins S4 and S5 such as *rpsD* (Figure 4). These mutations have tripled the error rate and have decreased growth rate by 35% (Mikkola and Kurland, 1988; Zaher and Green, 2010). However, accuracy also comes at a cost, and too much accuracy might hinder growth rate. Hyperaccurate streptomycin resistance (SmR) mutants often have altered ribosomal protein S12, such as *rpsL* (Figure 4), and may exhibit a 7-fold decrease in error rate (Zaher and Green, 2010). The decrease in error rate is correlated with growth rate decrease of up to 40% and longer elongation rates (Ehrenberg and Kurland, 1984; Kurland, 1992; Mikkola and Kurland, 1988). These observations suggest that, in order to optimize growth, cells must balance between the speed of translation and the error rate. In some scenarios, translational infidelity, caused by prions that promote stop codon readthrough in yeast, for example, may provide sequence plasticity that might be beneficial as the organism adapts to a new environment (Shorter and Lindquist, 2005).

Our theory predicts a resolution for the rate-specificity tradeoff of the decoding reaction. Given that the energy difference δ between cognate and noncognate pathways should be as large as physically possible (Figure 4), we showed that the difference between the GTP activation and codon recognition barriers, Δ_C, should be optimally about $-\delta/2$ (ranging between $-\delta$ and 0). This result defines a triangular region in the space of possible energy landscapes that is optimal for decoding. Several recent kinetic studies (Lee et al., 2007; Zaher and Green, 2010) indicate that the prokaryotic ribosome is indeed within this optimality region (Figure 4) (Supplemental Information, Tables S2, S3, and S4).

Our model suggests that the strong evolutionary pressure to improve ribosome decoding drove the energy landscape toward its current optimal shape. As a consequence, our analysis predicts that mutations in the ribosome will not significantly improve the wild-type decoding fitness. Even mutations that would provide higher decoding rate R_C or lower error fraction R_W/R_C (Ogle and Ramakrishnan, 2005) are expected to reduce the fitness or leave it practically unchanged. Kinetic studies of the "hyperaccurate" mutation *rpsD* and *rpsL* mutations reveal that, indeed, their decoding performance is, at best, similar to that of the wild-type (Figure 4). This holds also for ribosomes subject to antibiotic that exhibit a poor decoding relative to the wild-type (Gromadski and Rodnina, 2004b) (Figure 4 and Figure S1 available online; Experimental Procedures).

The simple effective energy landscape that we used in this work, with its distinct metastable states, was directly deduced from the experimental kinetic data. Single-molecule FRET studies, combined with computer simulations, suggest that this effective landscape is an approximation for a much more intricate energy landscape (Whitford et al., 2011b). In principle, similar optimality analysis could be applied also to a multiparameter fitness function on such an intricate landscape.

Enzymatic Reactions in the Presence of Competing Substrates

The analysis presented in this work can be generalized to more complicated decoding pathways with additional steps and branches and to other recognition systems. Moreover, it can be applied to the analysis of natural molecular recognition systems as well as to the design of artificial ones. For example, numerous enzymatic reactions, which can be described by MM kinetics, are often prone to substrate competition or inhibition (Fersht, 1985). If the kinetic rates of the competing reactions are known, our analysis gives a straightforward, testable prediction regarding the rates that yield optimal decoding (SI). In particular, we expect that the specificity will not saturate the maximal possible value to avoid a diminishing turnover rate. In the case when all competitor substrates associate at roughly the same rate k_{on} (as in the ribosome), the predicted specificity is about a square root of the maximal one, $S^* \approx S_{max}^{1/2}$(Figure 2D). Similar analysis can be applied to other cases. Another example is the rational design of drugs in which our analysis suggests a design principle to balance the tradeoff between maximizing the effect of a drug on its target while minimizing the side effect of interacting with competing targets.

EXPERIMENTAL PROCEDURES

tRNA Decoding Rates

The decoding rate is given by the rate of GTP hydrolysis, per ribosome per tRNA, at steady state:

$$R = \frac{k_1 k_2 k_3}{k_2 k_3 + k_{-1}(k_3 + k_{-2})}, \qquad \text{(Equation 5)}$$

where the kinetic parameters are according to the scheme in Figure 1. The rate per ribosome is $R \cdot [t]$, where $[t]$ is the *unbound* tRNA concentration. Because the rate constants are the exponents of the corresponding free energy barriers, $k \propto e^{-\Delta G}$, we rewrite R as

$$R = \frac{1}{\frac{1}{k_1} + \frac{1}{k_1}\cdot\frac{k_{-1}}{k_2} + \frac{1}{k_1}\cdot\frac{k_{-1}}{k_2}\cdot\frac{k_{-2}}{k_3}} \propto \frac{1}{e^{b_1} + e^{b_1}\cdot\frac{e^{-(b_1-s_2)}}{e^{-(b_2-s_2)}} + e^{b_1}\cdot\frac{e^{-(b_1-s_2)}}{e^{-(b_2-s_2)}}\cdot\frac{e^{-(b_2-s_3)}}{e^{-(b_3-s_3)}}} = \frac{1}{e^{b_1} + e^{b_2} + e^{b_3}} = \frac{1}{e^{B} + e^{b_3}}. \qquad \text{(Equation 6)}$$

Maximizing the Fitness Function

We consider a general performance measure ("fitness") F that is a function of the correct and wrong decoding rates, $[R_C(B, b_3), R_W(B, b_3, \delta)]$. The derivatives with respect to the various parameters are (using Equations 1 and 2)

$$\frac{\partial F}{\partial \delta} = -\frac{\partial F}{\partial R_W}\cdot R_W^2 \cdot e^{b_3+\delta} \qquad \text{(Equation 7.1)}$$

$$\frac{\partial F}{\partial B} = -\frac{\partial F}{\partial R_C}\cdot R_C^2 e^{B} - \frac{\partial F}{\partial R_W}\cdot R_W^2 e^{B} \qquad \text{(Equation 7.2)}$$

$$\frac{\partial F}{\partial b_3} = -\frac{\partial F}{\partial R_C}\cdot R_C^2 e^{b_3} - \frac{\partial F}{\partial R_W}\cdot R_W^2 \cdot e^{b_3+\delta} \qquad \text{(Equation 7.3)}$$

Biologically relevant measures F obey $\partial F/\partial R_C > 0$, $\partial F/\partial R_W < 0$ and therefore $\partial F/\partial \delta > 0$ (Equation 7.1). As a result, δ is expected to increase toward its biophysical limit. It is clear that the two derivatives, $\partial F/\partial B$ and $\partial F/\partial b_3$, in Equations 7.2 and 7.3 cannot vanish simultaneously. If $\partial F/\partial B$ (Equation 7.2) vanishes, then there is an extremum point in the B direction. In this case, $\partial F/\partial b_3$ (Equation 7.3) is always positive (because $\delta > 0$), and b_3 increases along the extremum line. If $\partial F/\partial b_3$ (Equation 7.3) vanishes, then there is an extremum point in the b_3 direction. In this case, $\partial F/\partial B$ (Equation 7.2) is always negative, and B decreases along the extremum line.

In the case of decoding, $F \propto R_C - d \cdot R_W$, the second derivative with respect to B is always positive, and thus the extremum point in the B direction is a minimum. Thus, F gets its maximal value at the upper boundary of δ and the lower boundary of B.

Solving $\partial F/\partial b_3 = 0$ (Equation 7.3) yields the implicit condition

$$\left(\frac{R_C}{R_W}\right)^2 = -e^{\delta}\frac{\partial F/\partial R_W}{\partial F/\partial R_C}. \qquad \text{(Equation 8)}$$

Taking the logarithm of condition (Equation 8), we find that the barrier that maximizes F is given by solving

$$\ln\left(\frac{R_C}{R_W}\right) = \frac{1}{2}\delta + \frac{1}{2}\ln\left|\frac{\partial F/\partial R_W}{\partial F/\partial R_C}\right|. \qquad \text{(Equation 9)}$$

Because $0 \le \ln(R_C/R_W) \le \delta$, the extremum always exist as long as $e^{-\delta} \le |(\partial F/\partial R_W)/(\partial F/\partial R_C)| \le e^{\delta}$.

The point $\ln(R_C/R_W) = \delta/2$ is exactly at the symmetric optimality condition, in the middle between the steepest points of the sigmoidal curves R_C and R_W (Figure 3A). Moreover, Equation 9 implies that the maximal point will remain in this symmetric region as long as $(4e^{\delta}/(1+e^{\delta})^2) \le |(\partial F/\partial R_W)/(\partial F/\partial R_C)| \le ((1+e^{\delta})^2/4e^{\delta})$. In other words, as

long as the both R_C and R_W are relevant to the fitness F—i.e., the respective derivatives $\partial F/\partial R_C$ and $\partial F/\partial R_W$ are not different by too many orders of magnitude—the maximal point is always in the symmetric region in between the steepest points of R_C and R_W (Figure 2). This result does not depend on the specific form of F. In the case of the ribosome, $e^{\delta} \approx 2 \cdot 10^5$, which defines a wide region of more than ten orders of magnitude.

Maximum of the Decoding Function

In the case of decoding, $F \propto R_C - d \cdot R_W$, the condition above (Equation 8) amounts to solving $(e^{b_3+\delta}+e^{B})^2/(e^{b_3}+e^{B})^2 = e^{\delta} d$. The barrier b_3 that provides maximal decoding is given by:

$$b_3^* = -\frac{1}{2}\delta + B + \ln\left(\frac{d^{1/2}e^{\delta/2}-1}{e^{\delta/2}-d^{1/2}}\right) \qquad \text{(Equation 10)}$$

The optimum exists as long as long as $e^{-\delta} < d < e^{\delta}$. For the ribosome, this regime is very wide, $5 \cdot 10^{-6} \approx e^{-12} < d < e^{+12} \approx 2 \cdot 10^5$. In this regime, Equation 10 is approximately linear in $\ln d$, $b_3^* \approx -(1/2)\,\delta + \mathrm{B} + (1/2)\ln d$.

Optimal Decoding—The Max-Min Solution

The minimal value of F is given by (Extended ExperimentalProcedures),

$$\min(F) = \begin{cases} e^{B}R_C = \dfrac{e^{B}}{e^{B}+e^{b_3}} & b_3 \geq -\dfrac{\delta}{2}+B \\ 1-e^{B}R_W = 1-\dfrac{e^{B}}{e^{B}+e^{b_3+\delta}} & b_3 \leq -\dfrac{\delta}{2}+B \end{cases} \qquad \text{(Equation 11)}$$

Maximizing the values of min(F) in (Equation 11) yields $b_3^* = -\delta/2 + \mathrm{B}$. Using the relation $B - b_2 = \ln(k_2 + k_{-1}/k_{-1}) = -\ln p$, we find that $\Delta_C^* = -\delta/2 - \ln p$ (Equation 3). Note that this value also maximizes the net rate $R_c - R_W$.

SUPPLEMENTAL INFORMATION

Supplemental Information includes Extended Experimental Procedures, one figure, and four tables and can be found with this article online at http://dx.doi.org/10.1016/j.cell.2013.03.032.

ACKNOWLEDGMENTS

We thank Marina Rodnina, Ada Yonath, Måns Ehrenberg, Jacques Ninio, Elisha Moses, Uri Alon, Rami Pugatch, Adam Lampert, Tamar Friedlander, Michel Springer, Tzachi Pilpel, Ron Milo, and Jean-Pierre Eckmann for valuable discussions. Y.S. is supported by the Human Frontier Science Program fellowship. T.T. thanks the Simons Foundation and Helen and Martin Chooljian for their generous support. T.T. is the Helen and Martin Chooljian Founders Circle Member in the Simons Center for Systems Biology of the Institute for Advanced Study, Princeton.

Received: October 12, 2011
Revised: October 3, 2012
Accepted: March 22, 2013
Published: April 11, 2013

REFERENCES

Bashan, A., and Yonath, A. (2008). Correlating ribosome function with high-resolution structures. Trends Microbiol. *16*, 326–335.

Blanchard, S.C., Gonzalez, R.L., Kim, H.D., Chu, S., and Puglisi, J.D. (2004). tRNA selection and kinetic proofreading in translation. Nat. Struct. Mol. Biol. *11*, 1008–1014.

Bouadloun, F., Donner, D., and Kurland, C.G. (1983). Codon-specific missense errors in vivo. EMBO J. *2*, 1351–1356.

Demeshkina, N., Jenner, L., Westhof, E., Yusupov, M., and Yusupova, G. (2012). A new understanding of the decoding principle on the ribosome. Nature *484*, 256–259.

De Vlaminck, I., van Loenhout, M.T., Zweifel, L., den Blanken, J., Hooning, K., Hage, S., Kerssemakers, J., and Dekker, C. (2012). Mechanism of homology recognition in DNA recombination from dual-molecule experiments. Mol. Cell *46*, 616–624.

Ehrenberg, M., and Kurland, C.G. (1984). Costs of accuracy determined by a maximal growth rate constraint. Q. Rev. Biophys. *17*, 45–82.

Ferreiro, D.U., Hegler, J.A., Komives, E.A., and Wolynes, P.G. (2011). On the role of frustration in the energy landscapes of allosteric proteins. Proc. Natl. Acad. Sci. USA *108*, 3499–3503.

Fersht, A.R. (1985). Enzyme Structure and Mechanism, Second Edition (New York: W. H. Freeman).

Fersht, A.R. (1998). Structure and Mechanism in Protein Science: A Guide to Enzyme Catalysis and Protein Folding (New York: W. H. Freeman).

Frank, J., Sengupta, J., Gao, H., Li, W., Valle, M., Zavialov, A., and Ehrenberg, M. (2005). The role of tRNA as a molecular spring in decoding, accommodation, and peptidyl transfer. FEBS Lett. *579*, 959–962.

Gromadski, K.B., and Rodnina, M.V. (2004a). Kinetic determinants of high-fidelity tRNA discrimination on the ribosome. Mol. Cell *13*, 191–200.

Gromadski, K.B., and Rodnina, M.V. (2004b). Streptomycin interferes with conformational coupling between codon recognition and GTPase activation on the ribosome. Nat. Struct. Mol. Biol. *11*, 316–322.

Gromadski, K.B., Daviter, T., and Rodnina, M.V. (2006). A uniform response to mismatches in codon-anticodon complexes ensures ribosomal fidelity. Mol. Cell *21*, 369–377.

Helstrom, C.W. (1995). Elements of Signal Detection and Estimation (Englewood Cliffs, NJ: PTR Prentice-Hall).

Herschlag, D. (1988). The role of induced fit and conformational changes of enzymes in specificity and catalysis. Bioorg. Chem. *16*, 62–96.

Hopfield, J.J. (1974). Kinetic proofreading: a new mechanism for reducing errors in biosynthetic processes requiring high specificity. Proc. Natl. Acad. Sci. USA *71*, 4135–4139.

Johansson, M., Lovmar, M., and Ehrenberg, M. (2008). Rate and accuracy of bacterial protein synthesis revisited. Curr. Opin. Microbiol. *11*, 141–147.

Johansson, M., Ieong, K.W., Åqvist, J., Pavlov, M.Y., and Ehrenberg, M. (2011). Rate and accuracy of messenger RNA translation on the ribosome. In Ribosomes, M.V. Rodnina, W. Wintermeyer, and R. Green, eds. (Vienna: Springer Vienna), pp. 225–235.

Johansson, M., Zhang, J., and Ehrenberg, M. (2012). Genetic code translation displays a linear trade-off between efficiency and accuracy of tRNA selection. Proc. Natl. Acad. Sci. USA *109*, 131–136.

Kurland, C.G. (1992). Translational accuracy and the fitness of bacteria. Annu. Rev. Genet. *26*, 29–50.

Lee, T.H., Blanchard, S.C., Kim, H.D., Puglisi, J.D., and Chu, S. (2007). The role of fluctuations in tRNA selection by the ribosome. Proc. Natl. Acad. Sci. USA *104*, 13661–13665.

Marshall, R.A., Aitken, C.E., Dorywalska, M., and Puglisi, J.D. (2008). Translation at the single-molecule level. Annu. Rev. Biochem. *77*, 177–203.

Mikkola, R., and Kurland, C.G. (1988). Media dependence of translational mutant phenotype. FEMS Microbiol. Lett. *56*, 265–269.

Munro, J.B., Sanbonmatsu, K.Y., Spahn, C.M., and Blanchard, S.C. (2009). Navigating the ribosome's metastable energy landscape. Trends Biochem. Sci. *34*, 390–400.

Ninio, J. (1975). Kinetic amplification of enzyme discrimination. Biochimie *57*, 587–595.

Ninio, J. (2006). Multiple stages in codon-anticodon recognition: double-trigger mechanisms and geometric constraints. Biochimie *88*, 963–992.

Ogle, J.M., and Ramakrishnan, V. (2005). Structural insights into translational fidelity. Annu. Rev. Biochem. *74*, 129–177.

Ogle, J.M., Brodersen, D.E., Clemons, W.M., Jr., Tarry, M.J., Carter, A.P., and Ramakrishnan, V. (2001). Recognition of cognate transfer RNA by the 30S ribosomal subunit. Science *292*, 897–902.

Ogle, J.M., Murphy, F.V., Tarry, M.J., and Ramakrishnan, V. (2002). Selection of tRNA by the ribosome requires a transition from an open to a closed form. Cell *111*, 721–732.

Pape, T., Wintermeyer, W., and Rodnina, M. (1999). Induced fit in initial selection and proofreading of aminoacyl-tRNA on the ribosome. EMBO J. *18*, 3800–3807.

Post, C.B., and Ray, W.J., Jr. (1995). Reexamination of induced fit as a determinant of substrate specificity in enzymatic reactions. Biochemistry *34*, 15881–15885.

Rodnina, M.V., and Wintermeyer, W. (2001). Fidelity of aminoacyl-tRNA selection on the ribosome: kinetic and structural mechanisms. Annu. Rev. Biochem. *70*, 415–435.

Savir, Y., and Tlusty, T. (2007). Conformational proofreading: the impact of conformational changes on the specificity of molecular recognition. PLoS ONE *2*, e468.

Savir, Y., and Tlusty, T. (2008). Optimal design of a molecular recognizer: molecular recognition as a Bayesian signal detection problem. IEEE J. Sel. Topics Signal Process. *2*, 390–399.

Savir, Y., and Tlusty, T. (2009). Molecular recognition as an information channel: the role of conformational changes. Information Sciences and Systems, CISS *2009*, 835–840.

Savir, Y., and Tlusty, T. (2010). RecA-mediated homology search as a nearly optimal signal detection system. Mol. Cell *40*, 388–396.

Schmeing, T.M., and Ramakrishnan, V. (2009). What recent ribosome structures have revealed about the mechanism of translation. Nature *461*, 1234–1242.

Schmeing, T.M., Voorhees, R.M., Kelley, A.C., Gao, Y.G., Murphy, F.V., 4th, Weir, J.R., and Ramakrishnan, V. (2009). The crystal structure of the ribosome bound to EF-Tu and aminoacyl-tRNA. Science *326*, 688–694.

Schuette, J.C., Murphy, F.V., 4th, Kelley, A.C., Weir, J.R., Giesebrecht, J., Connell, S.R., Loerke, J., Mielke, T., Zhang, W., Penczek, P.A., et al. (2009). GTPase activation of elongation factor EF-Tu by the ribosome during decoding. EMBO J. *28*, 755–765.

Schug, A., and Onuchic, J.N. (2010). From protein folding to protein function and biomolecular binding by energy landscape theory. Curr. Opin. Pharmacol. *10*, 709–714.

Shorter, J., and Lindquist, S. (2005). Prions as adaptive conduits of memory and inheritance. Nat. Rev. Genet. *6*, 435–450.

Villa, E., Sengupta, J., Trabuco, L.G., LeBarron, J., Baxter, W.T., Shaikh, T.R., Grassucci, R.A., Nissen, P., Ehrenberg, M., Schulten, K., and Frank, J. (2009). Ribosome-induced changes in elongation factor Tu conformation control GTP hydrolysis. Proc. Natl. Acad. Sci. USA *106*, 1063–1068.

Whitford, P.C., Geggier, P., Altman, R.B., Blanchard, S.C., Onuchic, J.N., and Sanbonmatsu, K.Y. (2010a). Accommodation of aminoacyl-tRNA into the ribosome involves reversible excursions along multiple pathways. RNA *16*, 1196–1204.

Whitford, P.C., Onuchic, J.N., and Sanbonmatsu, K.Y. (2010b). Connecting energy landscapes with experimental rates for aminoacyl-tRNA accommodation in the ribosome. J. Am. Chem. Soc. *132*, 13170–13171.

Whitford, P.C., Ahmed, A., Yu, Y., Hennelly, S.P., Tama, F., Spahn, C.M., Onuchic, J.N., and Sanbonmatsu, K.Y. (2011a). Excited states of ribosome translocation revealed through integrative molecular modeling. Proc. Natl. Acad. Sci. USA *108*, 18943–18948.

Whitford, P.C., Altman, R.B., Geggier, P., Terry, D.S., Munro, J.B., Onuchic, J.N., Spahn, C.M.T., Sanbonmatsu, K.Y., and Blanchard, S.C. (2011b). Dynamic views of ribosome function: energy landscapes and ensembles. In Ribosomes, M.V. Rodnina, W. Wintermeyer, and R. Green, eds. (Vienna: Springer Vienna), pp. 303–319.

Xia, T., SantaLucia, J., Jr., Burkard, M.E., Kierzek, R., Schroeder, S.J., Jiao, X., Cox, C., and Turner, D.H. (1998). Thermodynamic parameters for an expanded nearest-neighbor model for formation of RNA duplexes with Watson-Crick base pairs. Biochemistry *37*, 14719–14735.

Yarus, M., Valle, M., and Frank, J. (2003). A twisted tRNA intermediate sets the threshold for decoding. RNA *9*, 384–385.

Zaher, H.S., and Green, R. (2009). Fidelity at the molecular level: lessons from protein synthesis. Cell *136*, 746–762.

Zaher, H.S., and Green, R. (2010). Hyperaccurate and error-prone ribosomes exploit distinct mechanisms during tRNA selection. Mol. Cell *39*, 110–120.

Cell

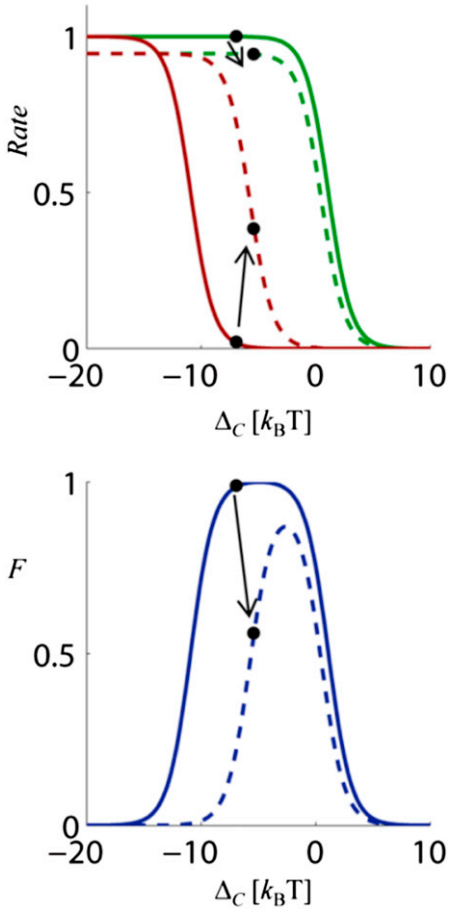

Figure S1. The Effect of Streptomycin on the Decoding Rates, Related to Figure 4

Normalized decoding rates and fitness for a correct codon (UUU) and a wrong one (CUC) as a function of the barrier difference Δ_C with (solid lines) and without (dashed lines) Streptomycin. *Top*: The correct rate R_C (green) slightly decreases while the wrong rate R_W (red) significantly increases due to the antibiotics. *Bottom*: The normalized fitness, $F \propto R_C - R_W$. Without antibiotics the measured barrier difference (black dot) is nearly optimal. The presence of antibiotics hampers the detection and the ribosome is shifted from optimality.

Normalized decoding rates and fitness for correct codon (UUU) and wrong one (CUC) as a function of the barrier difference Δ_C with (solid lines) and without (dashed lines) Streptomycin. *Top*: The correct rate R_C (green) slightly decreases while the wrong rate R_W (red) significantly increases due to the antibiotics. *Bottom*: The normalized fitness, $F \propto R_C - R_W$. Without antibiotics the measured barrier difference (black dot) is nearly optimal. The presence of antibiotics hampers the detection and the ribosome is shifted from optimality.